A new algorithm for the rotation of horizontal components of shear-wave seismic data

Kangan Fang and R. James Brown

ABSTRACT

Rotation of horizontal components of shear-wave data is one of the key processing procedures in anisotropy analysis. Several shear-wave rotation algorithms are available and suitable for different situations. In this paper, a new algorithm for the rotation of shear-wave data is proposed. This new algorithm can be used to rotate the horizontal components of shear-waves generated by multiple sources that have different amplitudes and wavelets in azimuthally anisotropic media. Synthetic data test and field data example showed that the algorithm are successful and robust.

INTRODUCTION

It is now commonly accepted that most upper-crustal rocks are anisotropic to some extent (Crampin, 1981). Anisotropy may be caused by fine layering in sedimentary rocks, by preferred orientation in crystalline solids, or by stress-aligned fractures or cracks (Crampin & Lovell, 1991). Shear-wave splitting is considered to be the most diagnostic phenomenon caused by anisotropy.

Shear-wave splitting may degrade the quality of the shear-wave data and cause mis-tie (Alford, 1986). We want to obtain the attribute information of anisotropy, such as natural polarization directions and degree of anisotropy, by analyzing shear-wave splitting. Through rotation, effect of anisotropy can be compensated for and the fast and slow shear-wave can be separated. In the case of azimuthal anisotropy caused by vertically-aligned fractures or cracks, the strike of fractures or cracks and the time lag of fast and slow waves can be determined by shear-wave rotation, which is of great interest to exploration geophysicists.

Several algorithms for the shear-wave horizontal component rotation have been invented. Alford's algorithm is devised especially for four-component rotation analysis and it can determine the orientation of the natural coordinate system (Alford, 1986). It requires that the two sources have the same wavelet signature. It has been shown that, for data acquired with a single source polarization, such as converted-wave data, Alford's rotation method does not work, without modifications (Thomsen, 1988).

Much work has been done using hodogram analysis methods to study S-wave splitting (e.g., Schulte and Edelmann, 1988). As discussed by Winterstein (1989), these methods require both very high signal-to-noise ratio and the presence of a single wavelet within the analysis window in order to be effective.

Other two-component birefringence-analysis schemes that do not involve hodograms have largely been based upon either the autocorrelation or crosscorreation of rotated components (Narville, 1986; Peron, 1990). Harrison (1992) presented an algorithm using the autocorrelation and crosscorrelation of rotated radial and transverse components, which is particularly suitable for converted waves and robust in the presence of noise.

The rotation algorithm presented here is similar to Alford's rotation algorithm, but it involves two parameters, the natural polarization direction angle and the time lag

between the fast and slow shear-waves, which can be determined by scanning, rather than only one parameter, the former, in Alford's rotation.

It can deal with the situation, where sources have different amplitudes and different wavelets. Synthetic data test and field data example showed that the algorithm is successful and robust.

PRINCIPLES

Shown in Figure 1, is a plan view of a multi-source, multi-receiver surface line for the situation where vertical S-wave splitting is assumed to occur. Each shear-wave source that does not coincide with the natural coordinate axes will split into a fast and a slow waves (Crampin, 1981; Thomsen, 1988). The S_1 direction indicates the polarization direction along which shear-waves travel at the fastest velocity β_1, while S_2 taken to be perpendicular to S_1, is the polarization direction along which S-waves travel at the slowest velocity β_2.

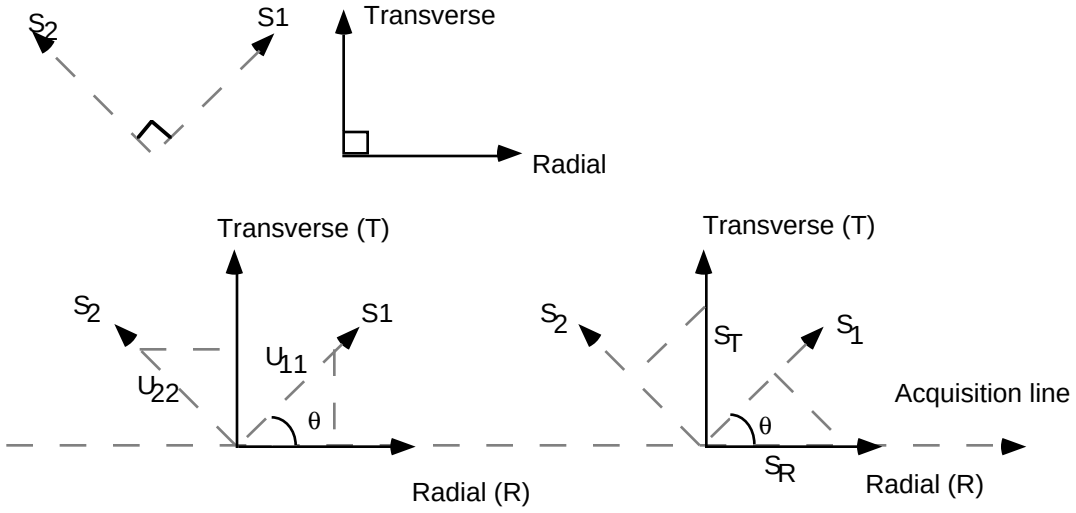

Figure 1. Illustration of multi-source, multi-receiver acquisition and shear-wave splitting.

$s_R(t)$ and $s_T(t)$ are the radial and transverse source along acquisition coordinate axes, respectively, and can be expressed as matrix:

$$S_a(t)=\begin{pmatrix} s_R(t) & 0 \\ 0 & s_T(t) \end{pmatrix} \tag{1}$$

both shear wave sources will split into shear-waves polarized in the S_1 and S_2 directions, which can be illustrated by Figure 2.

The relationship of splitting illustrated in Figure 2 can be expressed as matrix multiplication:

$$\begin{pmatrix} \cos\theta & \sin\theta \\ -\sin\theta & \cos\theta \end{pmatrix}\begin{pmatrix} s_R & 0 \\ 0 & s_T \end{pmatrix}=\begin{pmatrix} s_R\cos\theta & s_T\sin\theta \\ -s_R\sin\theta & s_T\cos\theta \end{pmatrix} \tag{2}$$

or

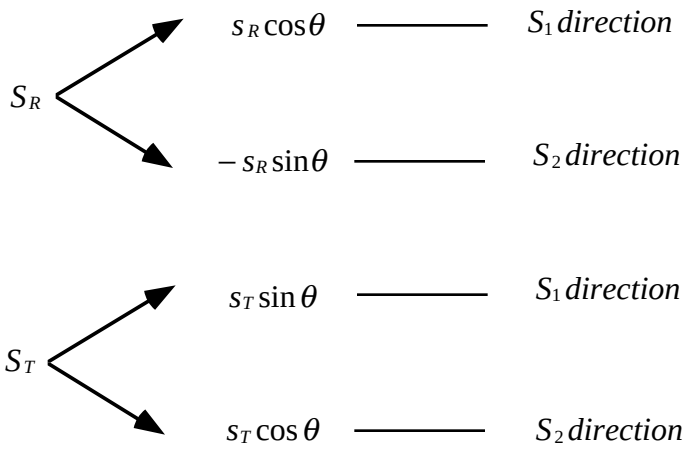

Figure 2. Illustration of the splitting of acquisition sources into fast- and slow-sources

$$R(\theta) \bullet S_a(t) = S(t) \tag{3}$$

where $R(\theta) = \begin{pmatrix} \cos\theta & \sin\theta \\ -\sin\theta & \cos\theta \end{pmatrix}$ is the vector rotation matrix and

$$R(-\theta) = R^{-1}(\theta) = R^{T}(\theta) = \begin{pmatrix} \cos\theta & -\sin\theta \\ \sin\theta & \cos\theta \end{pmatrix} \tag{4}$$

$S_a(t) = \begin{pmatrix} s_R & 0 \\ 0 & s_T \end{pmatrix}$ is the source matrix in the acquisition coordinate system, and

$S(t) = \begin{pmatrix} s_R\cos\theta & s_T\sin\theta \\ -s_R\sin\theta & s_T\cos\theta \end{pmatrix}$ is the source matrix in the natural coordinate system. Each row represents the components of the same direction.

Similarly, if $U(t) = \begin{pmatrix} u_{11} & 0 \\ 0 & u_{22} \end{pmatrix}$ is a data matrix in the natural coordinate system, where u_{11} and u_{22} are the reflected signals along S_1 and S_2 directions, respectively, then the data that would be recorded along acquisition coordinate system can be written as:

$$V(t) = R^{-1}(\theta) \bullet U(t) = \begin{pmatrix} u_{11}\cos\theta & -u_{22}\sin\theta \\ u_{11}\sin\theta & u_{22}\cos\theta \end{pmatrix} \tag{5}$$

Based on the above assumptions, we can write in frequency domain that:

$$R^{-1}(\theta) \bullet D(\omega) \bullet R(\theta) \bullet S_a(\omega) = V(\omega) \tag{6}$$

where, $D(\omega) = \begin{pmatrix} f_1(\omega)e^{-i\omega\delta_1} & 0 \\ 0 & f_2(\omega)e^{-i\omega\delta_2} \end{pmatrix}$ represents the travel time delay function of both fast and slow waves and $\delta 1$ and $\delta 2$ are the two way travel time of fast and slow wave respectively, f1 and f2 are the filter function for the fast and slow wave

propagation, respectively, which may account for the geometric spreading, attenuation and reflection coefficient, etc.

By rotation, we would like to have a data matrix that is generated by applying both sources and receivers along the natural coordinate system, i.e., the output data matrix of the rotation should be:

$$W(\omega) = D(\omega) \bullet S_a(\omega) = D(\omega) \bullet R^{-1}(\theta) \bullet D^{-1}(\omega) \bullet R(\theta) \bullet V(\omega) \qquad (7)$$

If $f_1(\omega) = f_2(\omega)$, equation (7) can be written as:

$$W(\omega) = \begin{pmatrix} w_{11} & w_{12} \\ w_{21} & w_{22} \end{pmatrix} =$$

$$\begin{pmatrix} \cos^2\theta + \sin^2\theta e^{+i\omega\Delta} & \sin\theta\cos\theta - \sin\theta\cos\theta e^{+i\omega\Delta} \\ \sin\theta\cos\theta e^{-i\omega\Delta} - \sin\theta\cos\theta & \sin^2\theta e^{-i\omega\Delta} + \cos^2\theta \end{pmatrix} \bullet \begin{pmatrix} v_{RR} & v_{RT} \\ v_{TR} & v_{TT} \end{pmatrix} \qquad (8)$$

where, in w_{ij} and v_{ij}, i represents the receiver direction and j represents the source direction, and $\Delta = 2z\left(\frac{1}{\beta_2} - \frac{1}{\beta_1}\right)$. Multiplication of $e^{i\omega\Delta}$ and $e^{-i\omega\Delta}$ in frequency domain is equivalent to time shift in time domain.

According to equation (8), if we can determine the angle between the direction of the polarization of fast shear wave and the acquisition line, θ, and the time lag between fast and slow waves, Δ, we can rotate the acquisition data matrix $V(t)$ into $W(t)$ to separate the fast and slow shear wave. These two parameters can be determined by scanning.

We rotate the input data matrix by a range of angles, θ, and time, Δ, and compute the norm on off-diagonal elements of rotated data matrix.

$$\left\| e_{ij}(\theta,\Delta,t) \right\|_p = \left(\sum_{k=1}^{N} \left| w_{ij}(\theta, t+k\Delta t) \right|^p \right)^{\frac{1}{p}} \qquad (9)$$

where N is the number of samples in the scanning window. Then we sum the norm on off-diagonal elements. If the θ and Δ are correct, the sum of the norms will be the minimum.

In the process described above, we do not need to assume that the wavelets and amplitudes of radial and transverse sources be the same.

SYNTHETIC DATA TEST

Figure 3 shows a synthetic data rotation example. Figure 3.a is the input data matrix generated by two sources with the same wavelet, both in main frequency and amplitudes. Figure 3.b is the result by our rotation algorithm, while Figure 3.c is the result by Alford's algorithm. Both methods work well when the two sources are the same. For synthetic data rotation test, we just create one CDP and we repeat this CDP 20 times for the purpose of display.

Figure 4 shows another synthetic data rotation test. Figure 4.a displays the input data matrix generated by sources with wavelets of the same type but different main frequencies and amplitudes. Figure 4.b and Figure 4.c are the results by our rotation algorithm and Alford's rotation, respectively. Our algorithm completely zeros the off-diagonal elements, but Alford's rotation leaves significant energy on the off-diagonal elements, because it requires that the sources have the same signature.

Figure 5 shows rotation with band-limited random noise added to the input data matrix. The mean amplitude of noise is 0.05 times that of signal. Figure 5.a is the input data matrix, while Figure 5.b is the rotation result of our algorithm, where the off-diagonal signal energy has been removed. This shows that the algorithm is robust in the presence of relatively strong noise.

Figure 6 shows the parameters (fast-wave polarization direction and time lag) scanning on the synthetic data without noise. The scanning is performed at regular time steps and the sum of norm of off-diagonal elements of the rotated data matrix is displayed in the form of contour, that can be used to pick up the desired parameters. Figure 6.a and 6.c demonstrate norm minimum of good resolution, because there are reflecting layers at the scanning times. And the parameters picked are exactly the same as those used to generate the data. As we move the scanning time away from the time at which there are reflectors, the norm minimum disappears and no parameters can be picked as illustrated by Figure 6.b and 6.d. This is the ideal case for parameter scanning. We always expect all kinds of noise in field data processing.

Figure 7.b shows the scanning result with noise added, where the mean amplitude of noise is 0.02 times that of signal, the norm minimum is still clear enough. But with increased noise, present scanning criterion does not give good resolution. Figure 7.a shows the scanning result without noise.

FIELD DATA EXAMPLE

Figure 8 shows two examples of scanning on field data. Because of the noise and the deviation of real situation from theoretical assumptions, such as that stack does not exactly represents zero offset data, we have good resolution and poor resolution scanning cases shown by Figure 8.a and 8.b, respectively. In the real rotation, other information about the natural polarization direction is needed.

Figure 9.a is a field data matrix before rotation from the area, Olds, Alberta, Canada. The mis-matched data elements demonstrated strong signal energy, which indicates that there should be azimuthal anisotropy. Figure 9.b is the rotated result, where the off-diagonal signal energy is greatly reduced and diagonal signal energy has been enhanced and the fast and slow waves have been separated. Only the data between 2400 ms and 2800 ms has been rotated and the other part of data is just for the purpose of display.

Figure 10.b displayed the fast and slow waves side by side to show the time lag between them. Figure 10.a is the input matched data elements shown in the same way as rotated data. Rotation separates the fast and slow waves and will improve the interpretation and also gives the information about the fractures or other anisotropic cause.

CONCLUSIONS

A new algorithm is presented based on a derivation that better describe the azimuthal anisotropy problem. By rotation scanning, two parameters, natural polarization

direction of fast wave and time lag between fast and slow waves, can be determined. The new algorithm can better deal with the data generated by the sources with different wavelet signatures and is robust in the presence of relatively strong noise. Synthetic data test and field data example are successful and reasonable.

There is also the potential to use it on single shear-source data (2-components) and for layer stripping.

ACKNOWLEDGMENTS

The authors would like to thank the CREWES sponsors for their support of this research.

REFERENCES

Alford, R. M., 1986, Shear data in the presence of azimuthal anisotropy: Dilley, Texas: 56th Internat.. Mtg., Soc. Expl. Geophys., Expanded Abstracts, 86, Session: s9.6.

Crampin, S, 1981, A review of wave motion in anisotropic and cracked elastic media: Wave motion, 3, 343--391.

Crampin, S. and Lowell, J., 1991, A decade of shear-wave splitting in the Earth's crust: what does it mean? what use can we make of it? and what should we do next? Geophys. J. Int., 107, 387-407.

Harrison, M.P., 1992, Processing of P-SV surface data: Anisotropy analysis, dip moveout, and migration: Ph.D thesis, The University of Calgary, Alberta, Canada.

Narville, C., 1986, Detection of anisotropy using shear-wave splitting in VSP surveys: requirements and applications: 56th Annual SEG meeting, Expanded Abstracts, 391-394.

Peron, J. 1990, Estimation of fracture directions from zero-offset VSP by two- and four- component rotation: 60th Annual SEG Meeting, Expanded Abstracts, 1443-1446.

Schulte, L., and Edelmann, H.A.K., 1988, Azimuthal anisotropy proven to be a useful approach for multicomponent shear-wave data processing: : 58th Internat.. Mtg., Soc. Expl. Geophys., Expanded Abstracts, 1156-1158.

Thomsen, L., 1988, Reflection seismology in azimuthally anisotropic media: Geophysics, 53, No. 3, 304-313.

Winterstein, D.F., 1989, Comparison of three methods for finding polarization direction of fast shear-wave: SEG research workshop, Snowbied, Utah, Technical Abstracts, 118-119.

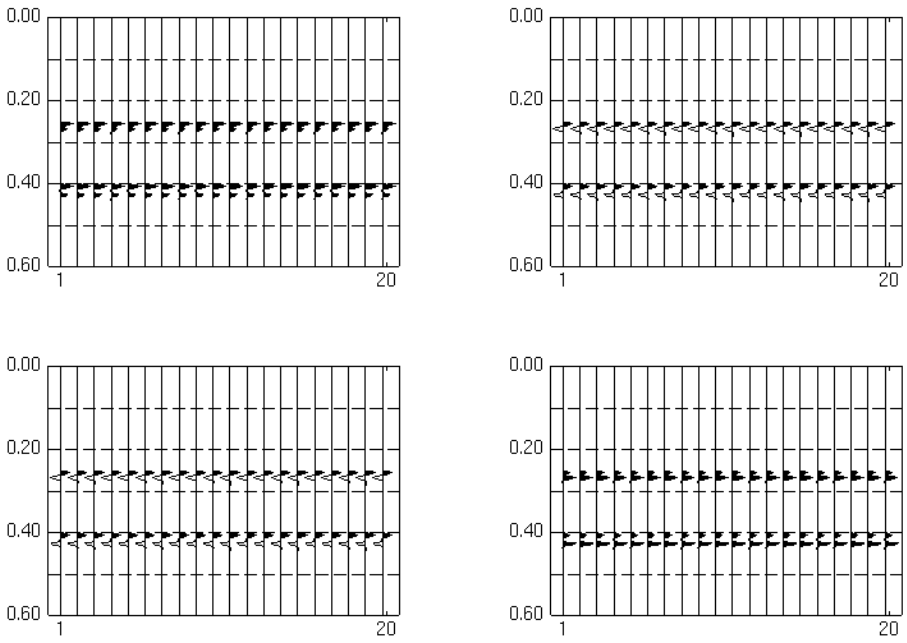

(3.a)

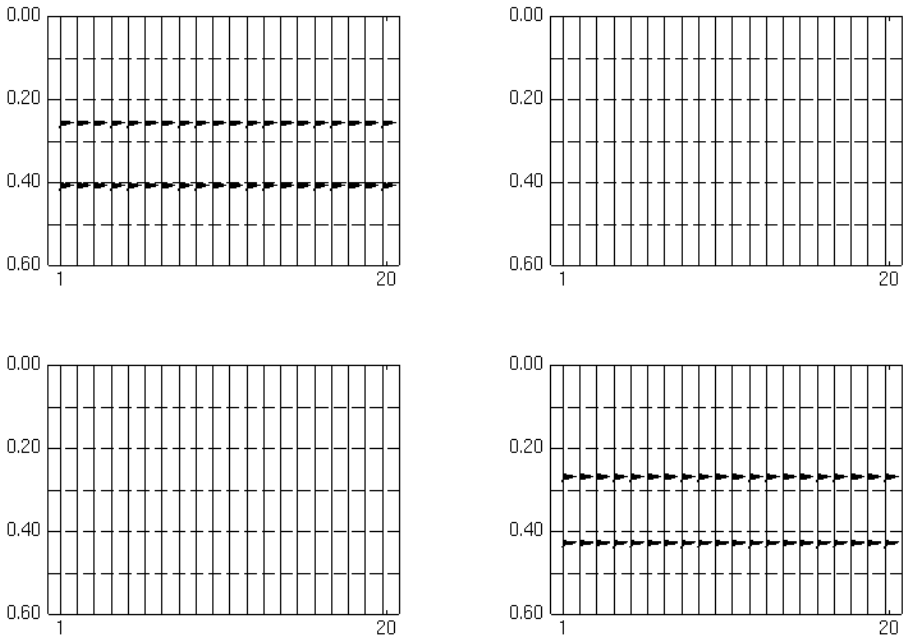

(3.b)

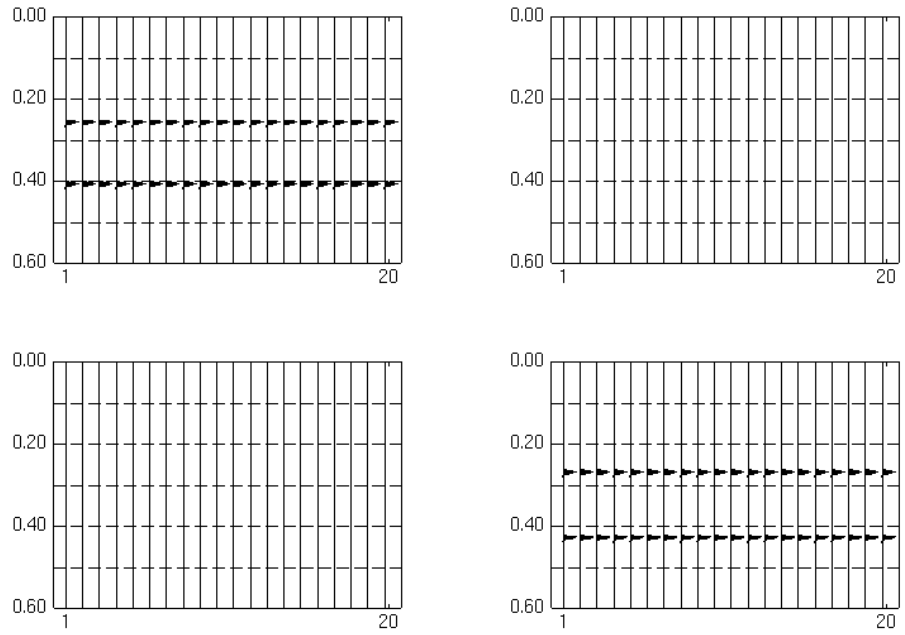

(3.c)

Figure 3. Synthetic data rotation showing (a) data matrix before rotation generated by the sources with the same wavelet signature; (b) data matrixr rotated by our algorithm; (c) data matrix rotated by Alford's algorithm

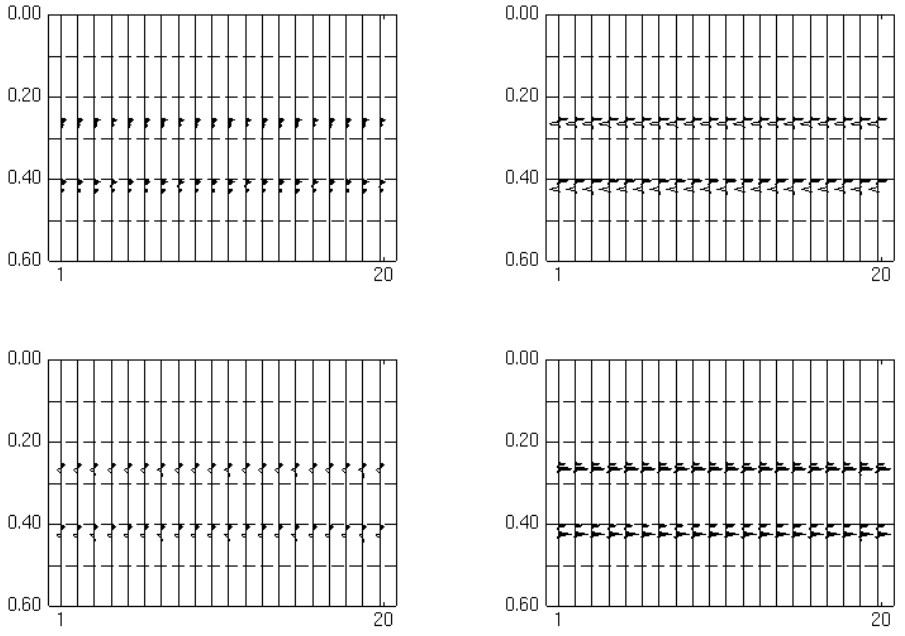

(4.a)

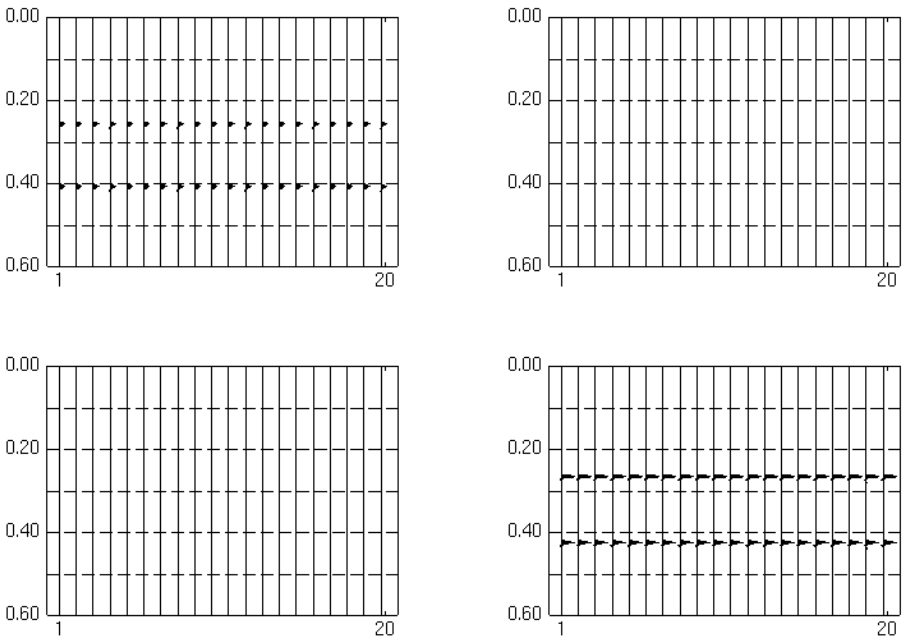

(4.b)

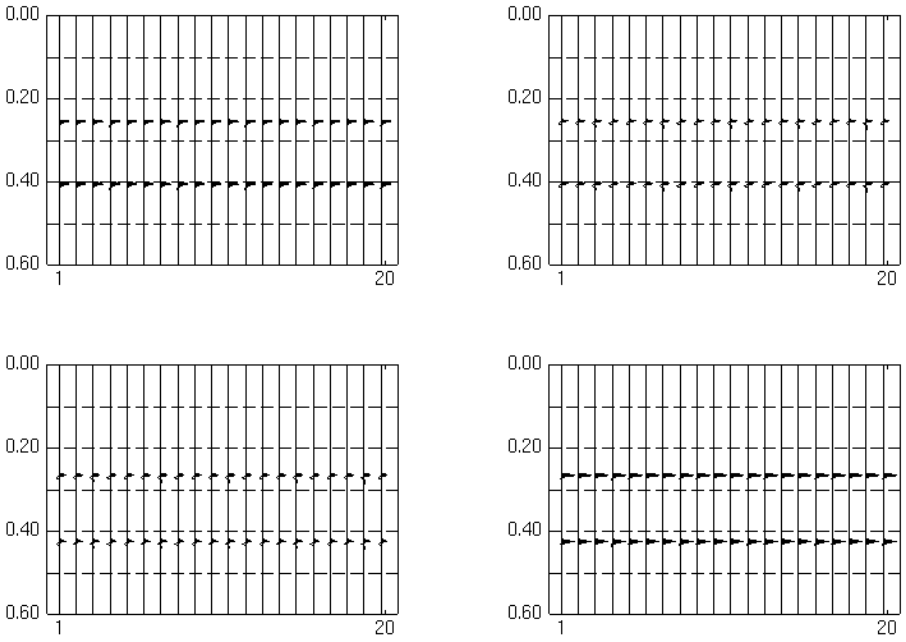

(4.c)

Figure 4. Synthetic data rotation showing (a) data matrix before rotation generated by sources with different wavelet frequency and amplitude; (b) data matrix rotated by our algorithm; (c) data matrix rotated by Alford's algorithm.

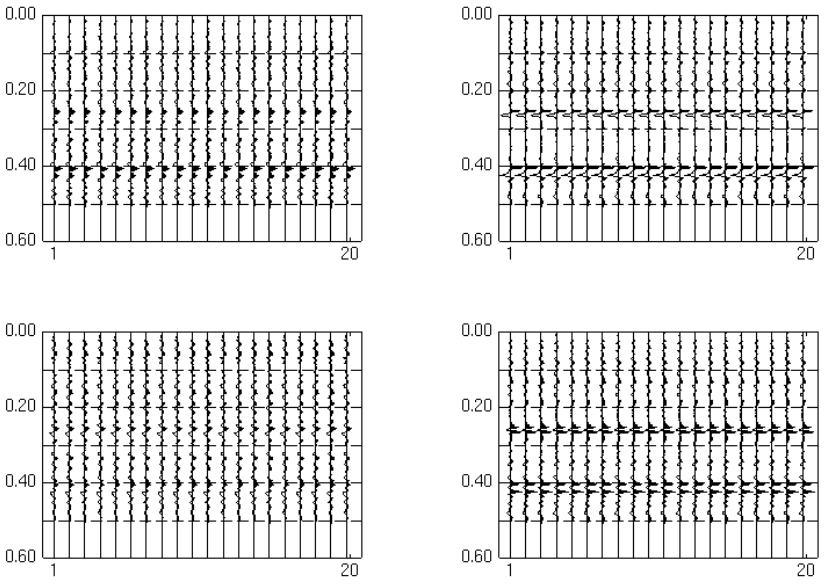

(5.a)

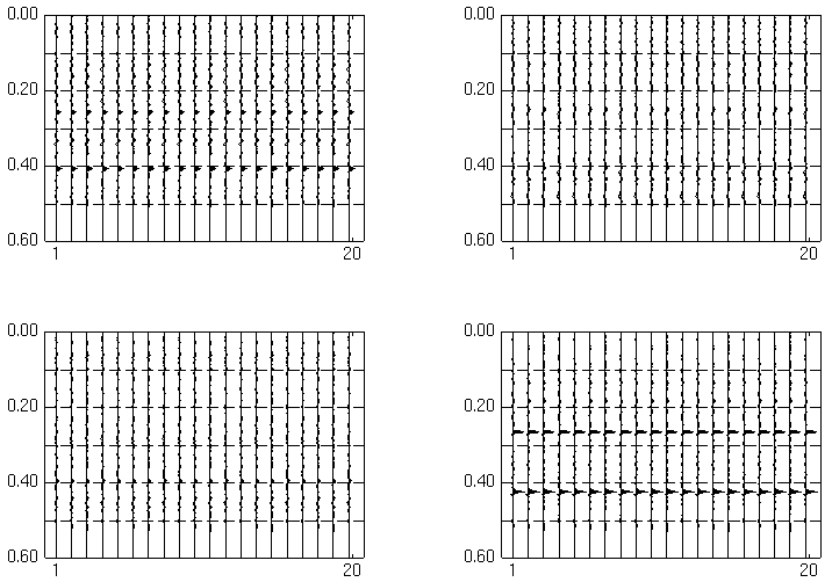

(5.b)

Figure 5. Rotation with noise added; (a) data matrix before rotation; (b) data matrix rotated by our algorithm.

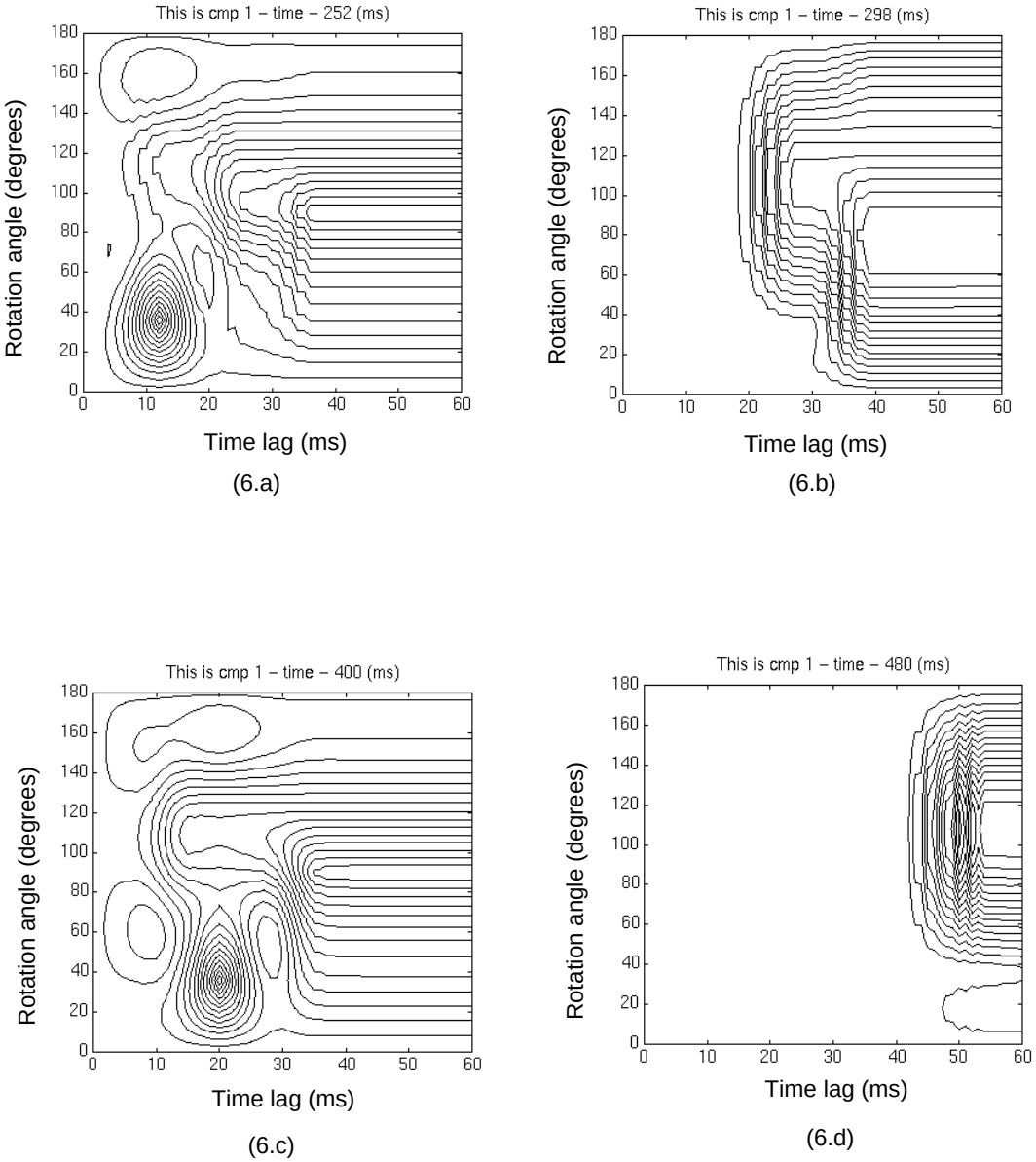

Figure 6. Synthetic data scanning at (a) 252 ms; (b) 298 ms; (c) 400 ms; (d) 480 ms.

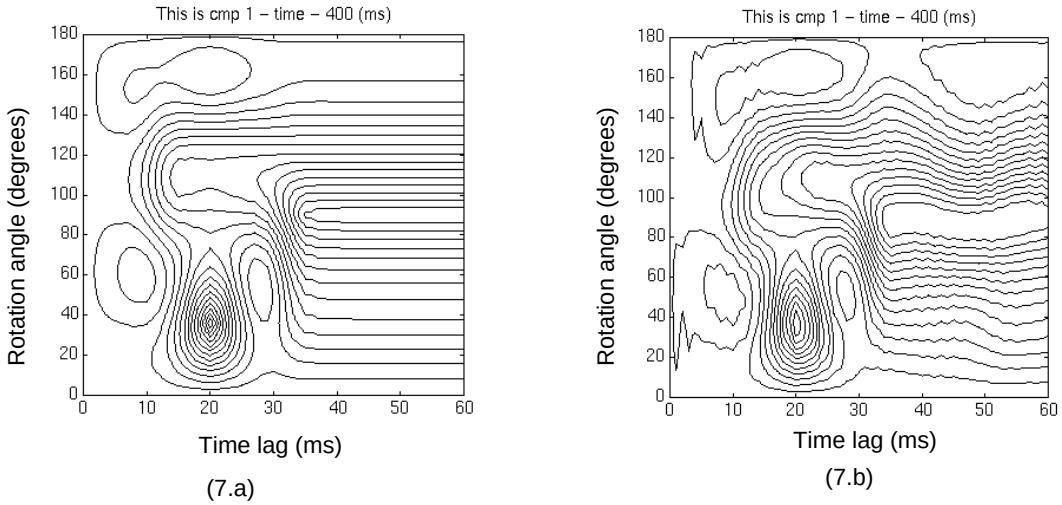

Figure 7. Scanning (a) without and (b) with noise added.

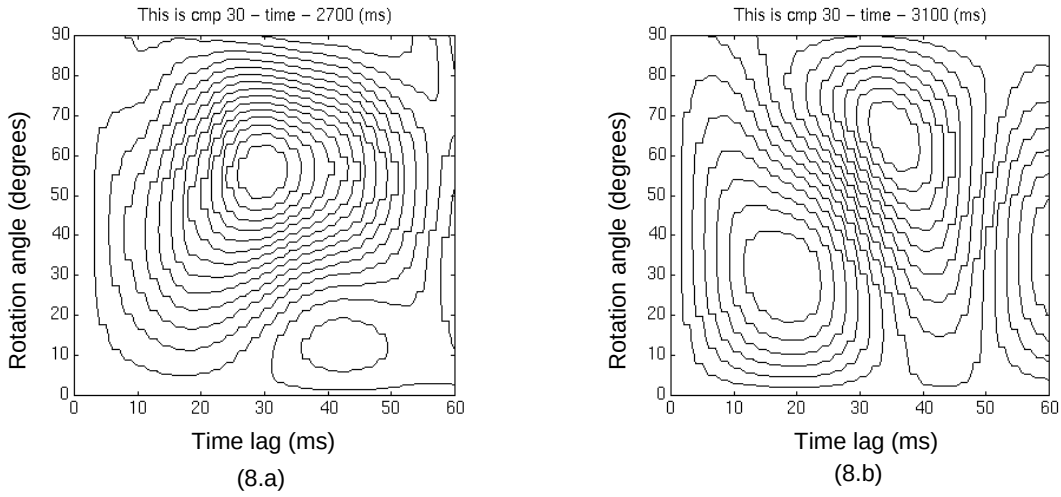

Figure 8. Scanning on field data; (a) good; (b) poor minimum concentration.

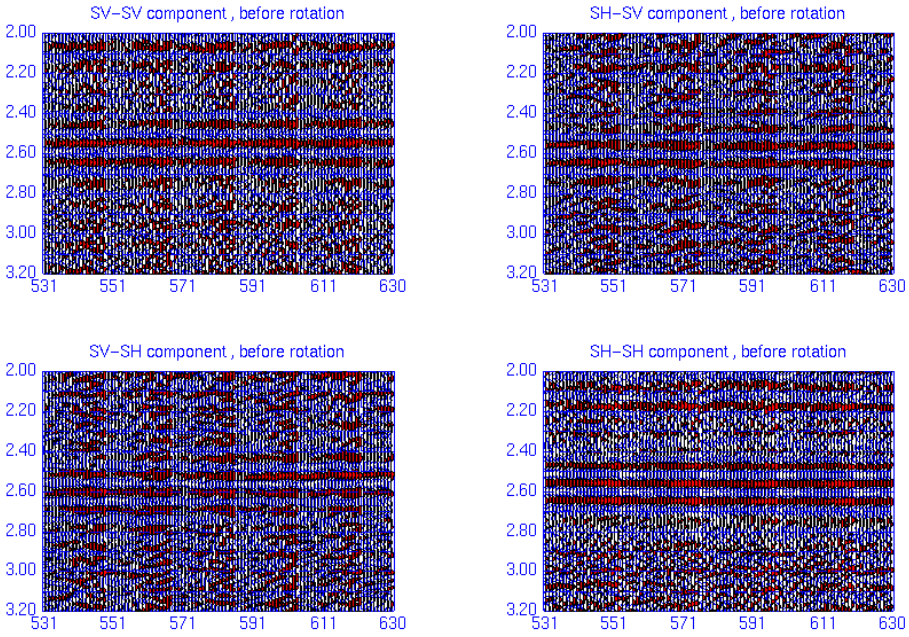

(9.a)

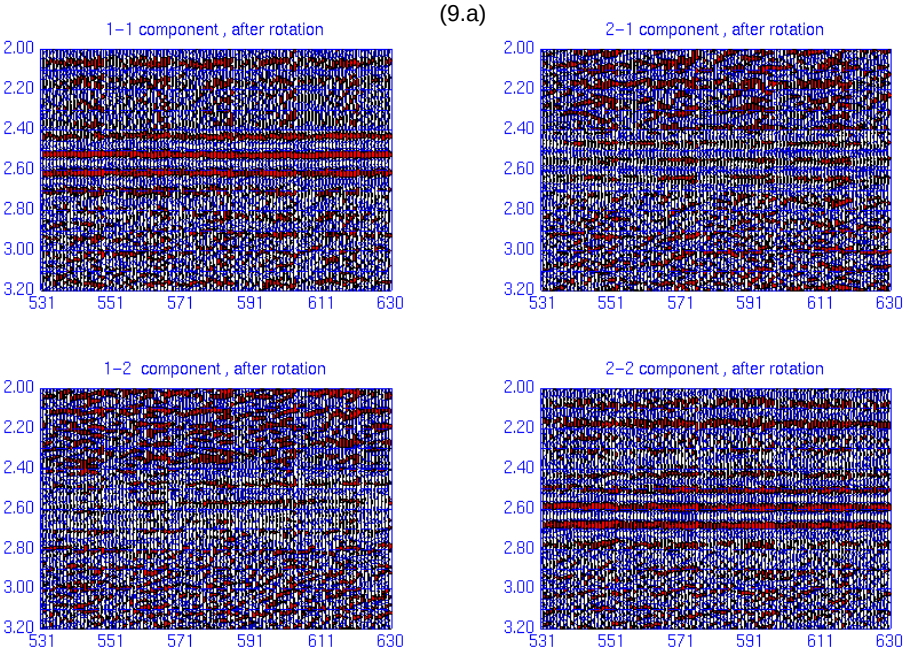

(9.b)

Figure 9. Field data rotation; (a) data matrix before rotation and (b) data matrix after rotation; only the part from 2.4 S to 2.8 S has been rotated.

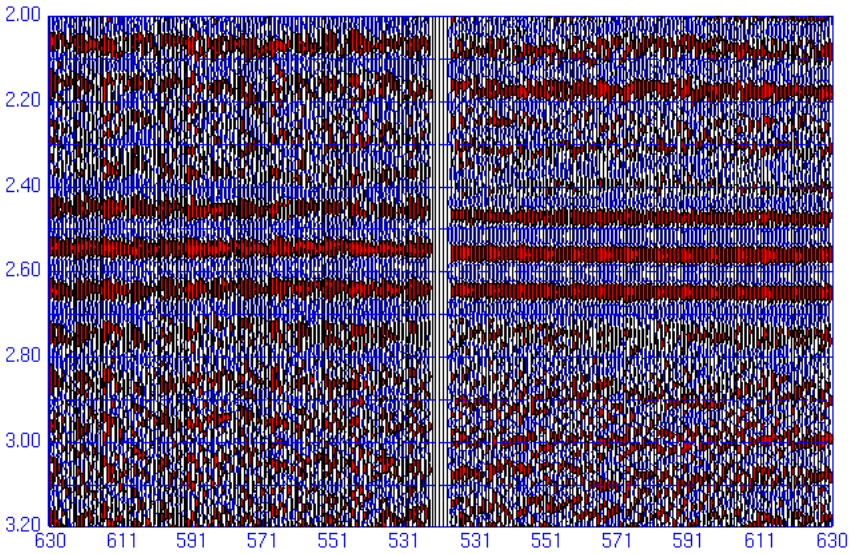

(10.a)

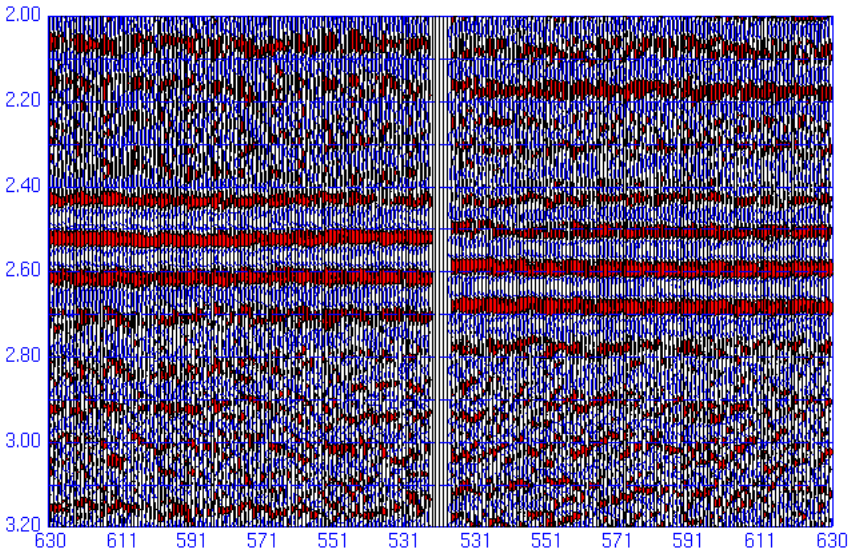

(10.b)

Figure 10. Field data rotation; (a) matched components (v-v and h-h) before rotation and (b) separated fast and slow waves after rotation.